Oecologia (2010) 164:1107–1119
DOI 10.1007/s00442-010-1770-6

GLOBAL CHANGE ECOLOGY - ORIGINAL PAPER

Stand-structural effects on *Heterobasidion abietinum*-related mortality following drought events in *Abies pinsapo*

Juan Carlos Linares · Jesús Julio Camarero · Matthew A. Bowker · Victoria Ochoa · José Antonio Carreira

Received: 3 April 2010 / Accepted: 21 August 2010 / Published online: 14 September 2010

Abstract Climate change may affect tree–pathogen interactions. This possibility has important implications for drought-prone forests, where stand dynamics and disease pathogenicity are especially sensitive to climatic stress. In addition, stand structural attributes including density-dependent tree-to-tree competition may modulate the stands' resistance to drought events and pathogen outbreaks. To assess the effects of stand structure on root-rot-related mortality after severe droughts, we focused on *Heterobasidion abietinum* mortality in relict Spanish stands of *Abies pinsapo*, a drought-sensitive fir. We compared stand attributes and tree spatial patterns in three plots with *H. abietinum* root-rot disease and three plots without root-rot. Point-pattern analyses were used to investigate the scale and extent of mortality patterns and to test hypotheses related to the spread of the disease. Dendrochronology was used to date the year of death and to assess the association between droughts and growth decline. We applied a structural equation modelling approach to test if tree mortality occurs more rapidly than predicted by a simple distance model when trees are subjected to high tree-to-tree competition and following drought events. Contrary to expectations of drought mortality, the effect of precipitation on the year of death was strong and negative, indicating that a period of high precipitation induced an earlier tree death. Competition intensity, related to the size and density of neighbour trees, also induced an earlier tree death. The effect of distance to the disease focus was negligible except in combination with intensive competition. Our results indicate that infected trees have decreased ability to withstand drought stress, and demonstrate that tree-to-tree competition and fungal infection act as predisposing factors of forest decline and mortality.

Keywords Basal-area increment · Climate change · Competition · Point-pattern analysis · Structural equation modelling

Communicated by Ram Oren.

Electronic supplementary material The online version of this article (doi:10.1007/s00442-010-1770-6) contains supplementary material, which is available to authorized users.

J. C. Linares (✉)
Departamento de Sistemas Físicos, Químicos y Naturales, Universidad Pablo de Olavide, Ctra. Utrera km. 1, 41002 Seville, Spain
e-mail: jclincal@upo.es

J. J. Camarero
ARAID, Instituto Pirenaico de Ecología (CSIC), Avda. Montañana 1005, Apdo. 202, 50192 Zaragoza, Spain

M. A. Bowker · V. Ochoa
Área de Biodiversidad y Conservación. Escuela Superior de Ciencias Experimentales y Tecnología, Universidad Rey Juan Carlos, C/Tulipán s/n, 28933 Móstoles, Spain

J. A. Carreira
Departamento de Biología Animal, Biología Vegetal y Ecología, Universidad de Jaén, Ed. B3, Paraje las Lagunillas s/n, 23071 Jaén, Spain

Introduction

Climate change may have effects on tree–pathogen interactions, with important implications for the dynamics of forest ecosystems (Desprez-Loustau et al. 2006). Of particular concern to date are potential increases in tree mortality associated with interactions of increasing rainfall variability and outbreaks of pathogenic fungi (Lindberg and Johansson 1992; Lonsdale and Gibbs 1996; Ayres and

Lombardero 2000). Understanding and predicting the consequences to forest ecosystems of these interactions are emerging as major challenges for global-change scientists (van Mantgem et al. 2009; Allen et al. 2010).

The pathogenicity of fungi is strongly influenced by environmental conditions. For instance, varying environmental conditions may modify the frequency of outbreaks and enhance sporulation and colonisation success (Ayres and Lombardero 2000; Desprez-Loustau et al. 2006). However, available results related to the interactive effects of drought and pathogens on forest trees were obtained mostly from experiments based on potted individuals or on plantations (see Desprez-Loustau et al. 2006 for a review). In comparison, studies based on mature individuals in natural forests are scarce, and few of them have considered interactions between stand structure and post-drought root-rot-related declines (but see Rayner 1986). Nevertheless, stand structure has been shown to modulate the consequences of climate change and root pathogens in certain tree species (Lewis and Lindgren 1999; Liu et al. 2007).

Trees of different sizes and crown classes compete differently for light, water and other resources within a stand (Peet and Christensen 1987; Orwig and Abrams 1997). Thus, depending on a stand's structural attributes, similar forest communities might exhibit different responses and ecological thresholds in the face of climate change-induced fungal pathogen outbreaks (Ayres and Lombardero 2000). Consequently, an assessment of the effects of drought stress and pathogen dynamics must consider stand structure in a spatially explicit context (Das et al. 2008; Olano et al. 2009). In this sense, point-pattern analyses allow the ability to reveal the scale and extent of mortality patterns and to test alternative hypotheses regarding the dynamics of disease spread (e.g. Solla and Camarero 2006). The spatial pattern may contain relevant information on the environmental factors acting to hasten the spread of a pathogen (Dobbertin et al. 2001; Holdenrieder et al. 2004; Liu et al. 2007).

Root-rot fungi, such as *Heterobasidion* species, have been reported in the literature to be associated with forest declines following severe droughts despite that their role as a decline factor was often inferred rather than well established (Rayner 1986; Ayres and Lombardero 2000). Several studies have suggested that *Heterobasidion* species become more aggressive on conifers subjected to water shortage (Puddu et al. 2003; Sánchez et al. 2005). Dendrochronology has been used to demonstrate the sequential association of droughts, radial-growth declines and invasion of woody tissues by root-rot fungi (Dobbertin et al. 2001; Cherubini et al. 2002). In addition, contrasting growth responses to drought stress among different crown-class trees might help us to understand their vulnerability to root-rot pathogens (Lewis and Lindgren 1999). Tree-to-tree competition also modulates tree response to water stress, as trees subjected to higher competition show lower radial growth and are more prone to die following extreme drought events (Linares et al. 2010). Therefore, this growth reduction could enhance tree vulnerability to root-rot pathogens.

To assess stand-structural effects on root-rot-related mortality following drought events, we analysed *Heterobasidion abietinum* mortality foci in Spanish stands of the relict fir *Abies pinsapo* Boiss. (Sánchez et al. 2005, 2007; Linares et al. 2009). Our null hypothesis was that the year of death of a tree (inferred from cross-dating of stem sections) is a function of the distance from the tree to the origin of the fungal infection (determined by the location of older root-rot stumps or dead trees). We also expected to find significant clustered spatial patterns for dead trees. We tested two alternative hypotheses: one, that post-drought tree mortality occurs more quickly than predicted by our null hypothesis; and two, that trees subjected to higher tree-to-tree competition are more prone to die. Our specific aims were (1) to describe and quantify the stand structure and spatial patterns of nearby *A. pinsapo* stands unaffected and affected by *H. abietinum* root-rot disease, (2) to quantify and compare the growth patterns of dead *A. pinsapo* trees subjected to root-rot disease and living trees not affected by the pathogen, and (3) to use spatially explicit competition estimates and precipitation data to model tree death. The fulfilment of these objectives will improve our current understanding of drought-induced and root-rot-related mortality events, and our ability to predict them.

Materials and methods

Climatic data

To estimate robust and long-term regional climatic records, local data from six nearby meteorological stations were combined into a regional mean for the period from 1920 to 2009 (see Supplementary materials). For each station, monthly total precipitation data were transformed into normalised standard deviations to give each station the same weight in calculating the average values for each month and year. To combine the data from each station, we used the MET routine from the Dendrochronology Program Library (Holmes 1992). In the study area, the estimated mean annual temperature is 11.6°C and the total annual precipitation is 1,089 mm. Because of the Mediterranean-type climate of our study sites, which are characterised by a marked summer drought, annual means were based on data from September of the previous year to August of the current year (Linares et al. 2010).

Field sampling and dendrochronological methods

Abies pinsapo Boiss. is a relict species whose small populations are restricted to coastal Mediterranean mountains in the Baetic (S. Spain) and Rifain (N. Morocco) ranges, mainly on north-facing slopes above 1,000 m a.s.l. (Linares and Carreira 2009). The study was carried out in natural stands of *A. pinsapo* located near the lower limit of the species' altitudinal range (for additional details, see Linares and Carreira 2009 and Linares et al. 2010). To describe and quantify the stand structure and spatial patterns of *A. pinsapo*, three stands unaffected by and three stands affected by *H. abietinum* root-rot disease were selected based on an extensive field survey (see Linares et al. 2009). The three disease foci (hereafter abbreviated as F plots) contained about 100 dead *A. pinsapo* trees each, while the three control stands (hereafter abbreviated as C plots) lacked visible symptoms of root-rot disease and were formed mainly of apparently healthy, living trees (Table 1). Within each plot (ca. 0.1 ha in size; located ca. 100 m apart), all trees with a diameter greater than 3 cm at 1.3 m (dbh) were identified, tagged and mapped, and dbh was measured. All trees were examined for symptoms corresponding to primary root-system rot caused by *Heterobasidion*, including fruiting bodies on the roots or stumps. In addition, the presence of bark beetles (*Scolytidae*) in the stems and the presence of crown damage were assessed (Supplementary materials). To quantify the growth patterns of *A. pinsapo* trees affected by root-rot disease, we randomly selected one of the three *H. abietinum* disease foci, and obtained stem cross-sections from all trees, including living and dead trees and, when possible, from stumps. Seventy-three trees were sampled for dendrochronological analyses.

The seventy-three cross-sections were taken at ca. 1.3 m (or slightly above that level in stems that showed wood rot at breast height). All samples were sanded until tree rings were clearly visible under a binocular microscope and visually cross-dated. Tree-ring widths were measured to the nearest 0.001 mm along two opposite radii per cross-section using a LINTAB measuring device (F. Rinntech, Heidelberg, Germany), and cross-dating quality was checked using COFECHA (Holmes 1983). Cross-sections were taken in February 2009, and we considered the last tree ring formed before 2008 in both cross-dated radii to represent the year of death. Mean master series for secondary growth were obtained from dominant trees from the control plots. The trend of decreasing ring width with increasing tree size was corrected by converting tree-ring widths into basal-area increments (BAI). Conversion of tree ring-widths to basal area increments was performed as follows: first, we calculated the stem basal area for the older tree-ring dated (TRW_1), located between the pit and the second tree-ring dated (TRW_2):

$$BA_1 = \pi^*(TRW_1)^2 \quad (1)$$

Then we calculated the stem basal area including the second tree-ring dated:

$$BA_2 = \pi^*(TRW_1 + TRW_2)^2 \quad (2)$$

Therefore, the first basal area increment value in our time series is:

$$BAI_1 = BA_2 - BA_1 \quad (3)$$

the second one is $BAI_2 = BA_3 - BA_2$, where $BA_3 = \pi^*(TRW_1 + TRW_2 + TRW_3)^2$, and so on.

Competition index

We estimated the tree-to-tree competition intensity (CI) that each focal tree was subjected to by calculating a distance-dependent competition index that takes into account the number and size of neighbours, and distance to neighbouring competitors (Hegyi 1974). The degree of competition experienced by the focal *i* tree was calculated as the sum over all *j* neighbouring trees within a radius *R* of the

Table 1 Structural characteristics of the study plots

Plot	Latitude (N)	Longitude (W)	Elevation (m a.s.l.)	Area (m^2)	Mean dbh of living trees/dead trees/stumps (cm)	Mean age (years)[a]	Density (ind. ha^{-1})	Basal area (m^2 ha^{-1})	Basal area of living trees/dead trees/stumps (%)
C1	36°43′27″	4°58′01″	1,181	982	17.10/20.20/–	50 ± 2.4	1,314	37.64	96.84/3.16/0
C2	36°43′26″	4°58′03″	1,199	905	17.72/11.13/–	48 ± 1.6	1,425	46.93	97.88/2.12/0
C3	36°43′30″	4°58′06″	1,200	852	12.86/9.00/–	52 ± 1.3	2,535	39.90	91.95/8.05/0
F1	36°43′29″	4°58′04″	1,190	1,256	24.15/18.22/13.58	38 ± 1.5	828	31.08	58.58/33.95/7.47
F2	36°42′15″	4°57′29″	1,111	1,256	14.87/14.22/14.83	n.d.	804	15.51	61.07/35.89/3.04
F3	36°42′19″	4°57′25″	1,070	1,256	15.52/14.46/8.00	n.d.	788	17.16	57.50/42.02/0.47

Values are mean ± SE

[a] Age estimated at 1.3 m

quotients between the basal-area ratio BA_j/BA_i and the distance between the focal tree i and the corresponding neighbouring tree j ($dist_{ij}$):

$$CI = \sum_{j=1}^{N(R)} (BA_j/BA_i)/dist_{ij} \quad (4)$$

The threshold radius above which neighbours were regarded as not competing was 8 m (see Linares et al. 2010).

Spatial analyses

To analyse the spatial pattern of tree classes, we used the pair-correlation function $g(t)$ (Diggle 2003). We performed univariate ($g(t)$) and bivariate ($g_{12}(t)$) point-pattern analyses to characterise the spatial distributions and associations, respectively, of living and dead trees. In the univariate case, we analysed the extent to which events show departure (aggregation or regularity) from complete spatial randomness (CSR), in which case $g(t) = 1$. Values of $g(t)$ greater or less than 1 indicate clustering or overdispersion, respectively. In the bivariate case, values of $g_{12}(t)$ greater or less than 1 indicate attraction or repulsion, respectively. We carried out the spatial analyses up to 10 m with a 1-m resolution. Because first-order effects due to environmental heterogeneity may obscure second-order effects related to tree-to-tree spatial interactions, the selection of a null model is relevant. We used heterogeneous Poisson processes as null models because they would retain the large-scale structure of the pattern but remove its local heterogeneity (Stoyan and Stoyan 1994). In the bivariate analyses, we used the random labelling null model to investigate whether dead trees are randomly distributed within the combined pattern of dead and living trees (Goreaud and Pèlissier 2004). Finally, tests of significance were constructed using 999 Monte Carlo simulations, estimating the rejection limits as the 5 lowest and 95 highest simulated values for each distance. The simultaneous testing of several distances may increase Type-I error, leading to the rejection of the null model even if it is true. Hence, we used a goodness-of-fit test (GOF) to summarise the total squared deviation between the observed pattern and the theoretical results across the distances analysed in the univariate analyses (Diggle 2003). Point-pattern spatial analyses were performed using the software Programita (Wiegand and Moloney 2004).

Data analyses and mortality modelling

We assumed that the disease originated at a single point by airborne basidiospores that germinated on fresh stumps or in stem or root wounds on the surfaces of living trees (see Supplementary materials). We also assumed that disease dispersal occurred mainly by direct growth of the pathogen from tree to tree through root contacts or grafts and therefore that dispersal pattern might be modelled as a function of distance from the infection foci. Hence, tree infection and death should occur more quickly if groups of trees show clustered spatial patterns. On the other hand, drought events in the past 20 years, in concert with tree-to-tree competition, have severely reduced the radial growth of *A. pinsapo* (Linares et al. 2010). These phenomena may have intensified the pathogenicity of the disease or favoured their spread. Thus, tree mortality may occur more quickly than predicted by a simple distance model for trees subjected to more intensive competition following drought events.

We used a structural equation modelling (SEM) approach to analyse our data as a system of variables and to partition the effects of multiple correlated factors that might affect tree mortality (Grace 2006). We first constructed an a priori model of our system wherein tree competition, drought severity, distance to disease origin, and all possible second-order interactions had direct effects upon the year of death derived from dendrochronological cross-dating of dead trees. As a simple index of drought severity, we summed the annual precipitation recorded for the year of death and the previous 2 years. Preliminary regression analysis indicated that this simple climatic variable was more informative than including separate climatic variables or summarising them in a multivariate construct (data not shown). To improve normality, we log-transformed competition values; however, some variables could not be transformed. We used Akaike's information criterion (AIC) to select among a set of six nested models of varying complexity reduced from this global model (Burnham and Anderson 2002). Our six models included: (1) an "independence" model, which hypothesised that none of the predictors was related to the year of death; (2) a "null" model, which stated that distance from the disease origin was the best predictor of the year of death; (3) a "competition-distance" model, which stated that the year of death was a function of distance from disease origin, competition index, and their interaction; (4) a "precipitation-distance" model, which stated that the year of death was a function of distance from disease origin, total precipitation of the previous 3 years, and their interaction; (5) a "main-effects" model, which stated that the year of death was a function of distance from disease origin, precipitation, and competition; and (6) a "global model", which stated that these three factors and their second-order interactions determined the year of death. The interaction terms were estimated by centering the main effects (subtracting the mean values from each value) and obtaining the cross-products of the two interacting main effects (Kline and Dunn 2000). In all models containing

interaction effects, main effects were specified to affect their corresponding interaction terms to account for the fact that interactions are mathematically derived from main effects. Also, in models with more than one main effect, main effects were allowed to correlate to accommodate the common occurrence in field data of non-zero correlations among predictor variables which arise due to chance alone.

The model with the lowest AIC value was selected as the best model (Burnham and Anderson 2001). The AIC approach permits relative assessment of models in a set but does not inform us about the absolute quality of a model. To obtain information about the absolute fit of the best model, we estimated path coefficients and performed associated probability tests for the best model and performed overall goodness of fit tests (Grace 2006). The goodness of fit test estimates the probability that the data fit the model structure; thus, a high probability value indicates that a model is a highly plausible causal structure underlying the observed correlations. Because some variables violated the normality assumption, we also verified our results using a more robust bootstrap test. After selection of the best model, and testing of its absolute fit, we used the knowledge gained from the model selection process to edit some information from the best model to construct a post-hoc model. A post-hoc model can be viewed as a provisional improvement over the best model, which requires confirmation in future investigations (Burnham and Anderson 2001; Grace 2006).

Results

Stand structure and spatial patterns

The six studied plots showed high stand density, dominated by trees with dbh less than 25 cm (Fig. 1; Table 1) and scattered large trees at very low density (about 10 trees ha^{-1} for dbh around 85 cm; Fig. 1). Mean stand density was significantly higher in the unaffected plots (C), likely because in the mortality-foci plots (F), several dead trees and older stumps could not be measured due to advanced wood decay. Plot C3 showed the highest percentage of dead trees unrelated to root-rot. Synergistic effects of drought and tree competition due to high stand density (more than 2,500 trees ha^{-1}) appeared to be the most likely factor to explain this mortality. F plots contained numerous standing and windthrown dead trees related to root-rot disease, and *Heterobasidion* fruiting bodies were identified in some windthrown trees and stumps (Supplementary materials). Basal area of dead trees in the mortality foci ranged from 34 to 42%, and basal area of stumps ranged from 1 to 8%. In control plots, basal area of dead trees ranged from about 2 to 8%, and stumps were absent (Table 1). F plots contained an average of more than 300 dead trees per ha; about 80% of the dead trees belonged to the 15–25 cm dbh size classes.

Most of the analysed univariate patterns in the unaffected plots did not significantly differ from spatial randomness (Table 2; Fig. 2). However, the *Heterobasidion*-affected F plots showed significant clustering at short (2–3 m) and intermediate distances (5–7 m), mainly due to the aggregated pattern of dead trees. The bivariate analyses of living and dead trees in F plots did not show significant global spatial patterns because goodness-of-fit test (GOF) was not significant (Fig. 3). However, living and dead trees in the F1 plot showed a trend toward repulsion at short distances (1–4 m).

Temporal climate-driven patterns and tree growth

Annual rainfall data for the study area showed both rainy years (1990, 1996 and 2001) and years characterised by severe droughts (1995, 1999 and 2005) superimposed over a long-term declining trend (Fig. 4a). Mean basal-area increment (BAI) master series obtained from dominant trees in the control plots indicated an increase in relative growth rate before the 1980s. Growth decline began in all of the studied trees between the late 1980s and the early 1990s (Fig. 4b). Sharp growth reductions occurred in 1981, 1995 and 1999. Mean BAIs for trees that died between 1992 and 2001 had decreased significantly since the onset of the 1980 s (i.e. about 10–20 years prior to their death). The mean BAI of trees that died between 2002 and 2007 was similar to that of currently living trees and was strongly correlated ($r = 0.87$; $P < 0.01$) with the master series (Fig. 4b). Living trees yielded lower mean BAIs than the master series between 1970 and the onset of the 1990s, likely due to elevated stand density and competition. As the 1990s progressed, BAI differences among several tree classes narrowed. Beginning in 1997, the mean BAI of currently living trees located within the mortality foci became even larger than that of dominant trees in control plots, likely as a response to reduced competition following the death of neighbouring trees.

Structural equation modelling

The global model was selected as the best model (Fig. 5). It was the only one that included both the main effects of precipitation and competition and the interaction effect of distance from origin × competition. These effects were all highly significant ($P < 0.001$) and together explained 61% of the total variance in year of death (see Supplementary data). The effect of precipitation was noteworthy because of its strength and negative effect ($r = -0.63$), which indicated that high precipitation periods accelerated

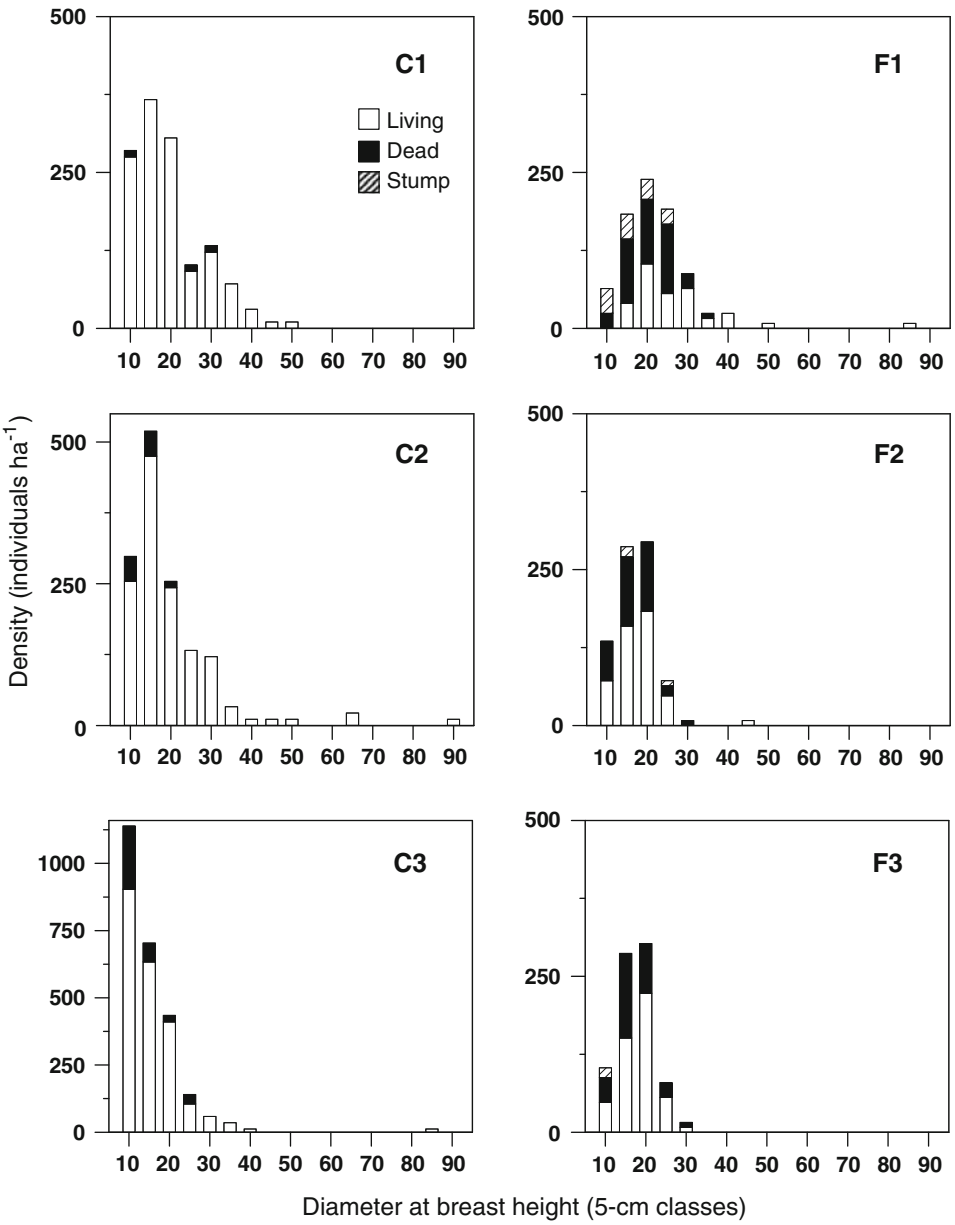

Fig. 1 Frequency distribution of diameter at 1.3 cm (dbh) of *Abies pinsapo* stands unaffected (plots *C1*, *C2* and *C3*) and affected (plots *F1*, *F2* and *F3*) by *H. abietinum* root-rot disease. *Empty*, *black* and *shaded areas* represent living trees, dead trees, and stumps, respectively. Note the larger density scale for plot *C3*

mortality. Competition intensity was also negatively related to the year of death, which indicated that high tree-to-tree competition accelerated mortality (Fig. 5). Notably, the effect of distance to the focus of infection depended on the competition intensity to which the tree was subjected (see Supplementary data). Finally, the selected model generated plausible predictions of the observed spatio-temporal mortality patterns (Figs. 5, 6).

Although the global model was the best of the model set, its absolute fit was poor ($\chi^2 = 17.2$, $P = 0.008$, RMSEA = 0.16, $P = 0.02$, Bootstrap $P = 0.32$; note: low P values indicate poor goodness of fit). The reason for the poor fit was because the model did not specify a correlation which existed between two of the interaction terms (distance to origin × precipitation and precipitation × competition). This correlation arose because both terms are partially mathematically-derived from precipitation data, and does not represent a substantive departure in the results or interpretation of the model.

As a means of guiding future research, we constructed a post-hoc modification of the best model which eliminated predictors which appeared to be uninformative in all models examined (See Supplementary data): distance to origen, distance to origen × precipitation, and precipitation × competition. The goodness-of-fit was excellent by all criteria ($\chi^2 = 0.34$, $P = 0.85$, RMSEA = 0.00, $P = 0.866$, Bootstrap $P = 0.88$), the model was much more parsimonious than the best model, and the variance

Table 2 Univariate (living, dead, and living plus dead trees) spatial patterns of *A. pinsapo* trees based on the pair-correlation function $g(t)$

Plot	Type of trees	n	GOF	P	Distance (m)									
					1	2	3	4	5	6	7	8	9	10
C1	Living	121	666	0.33	•	•	•	•	•	•	•	•	•	•
C2	Living	129	387	0.61	•	•	•	•	•	•	•	•	•	•
C3	Living	140	893	0.11	•	•	+	•	•	•	•	•	•	•
F1	Living + dead	104	964	0.04	•	+	•	•	•	•	•	•	•	•
F2	Living + dead	102	998	0.01	•	•	+	•	+	•	+	•	•	•
F3	Living + dead	98	955	0.04	•	•	+	•	•	•	•	•	•	•
F1	Living	37	134	0.87	•	•	•	•	•	•	•	•	•	•
F2	Living	59	929	0.07	•	•	•	•	•	•	•	•	•	•
F3	Living	63	707	0.29	•	•	+	•	•	•	•	•	•	•
F1	Dead	67	993	0.01	•	+	•	•	•	•	+	•	•	•
F2	Dead	43	778	0.22	•	•	•	•	•	•	+	•	•	•
F3	Dead	35	419	0.58	•	•	•	•	•	•	•	•	•	•

The goodness-of-fit test (GOF) and its associated probability (P) summarise the deviation between the observed and simulated patterns, with higher values of GOF indicating stronger spatial patterns. Statistically significant values at the 95% level are indicated by (+) for clustering, and (•) indicates a pattern not significantly different from spatial randomness

n is the number of trees analysed

explained in year of death was only slightly less ($R^2 = 0.59$; Fig. 7). This modified model does not replace the best model, rather it suggests a model form which should be included in future model selection procedures or confirmed using a hypothesis testing approach (Grace 2006).

Discussion

Predisposing, inciting, and contributing stressors in *Abies pinsapo* mortality events

Tree decline can be theoretically envisioned as a sequential process of predisposing, inciting, and contributing stressors (Manion 1991). Drought has often been considered an inciting factor; whereas root pathogens, such as *Heterobasidion* species, have been considered a contributing factor (Desprez-Loustau et al. 2006). However, in many cases, this conceptual model has proven difficult to demonstrate or even to assess in the field. Alternative hypotheses, such as a lower ability of infected trees to withstand stress (with infection playing the role of a predisposing decline factor), are also feasible. We hypothesised that tree mortality occurs more rapidly than predicted by a simple distance model including a high tree-to-tree competition following drought events. Our results indicate that infected trees have decreased ability to withstand drought stress and demonstrate that tree-to-tree competition and fungal infection act as predisposing factors in their decline and mortality. Tree-to-tree competition and proximity to more trees which may be infected is a predisposing factor because it could enhance physiological vulnerability to fungal pathogens and also allows more potential exposure to infected trees. If fungal infection does occur, host mortality is greatly enhanced by wet weather-promoted spread of the pathogen through the tree. So, wet weather or climatic variability must be a contributing factor, since they act in concert with a pre-existing fungal infection.

Is drought or climatic variability the principal stressor in tree mortality?

Direct effects of drought on pathogens are generally negative because most fungi require free water or high moisture for spore dispersal, germination and infection (Lacey 1986). Indeed, we found a negative relationship between annual precipitation and the year of tree death (Fig. 5). This finding suggests that root-rot-related mortality is favoured by moister conditions. Although most fungal pathogens exhibit substantial plasticity and can grow at water potentials well below the minimum needed for growth of their host plants, moisture is indispensable for mycelial growth within the host (Korhonen and Stenlid 1998). Attenuation of the activity of decay fungi by both high and low moisture content of wood, in dead timber as well as in living trees, is well established (Rayner 1986). Wood moisture has also been shown to be an important factor in determining the success of infections of Sitka spruce (*Picea sitchensis*) stumps by *Heterobasidion annosum*, with an optimum at 30–70% saturation (Redfern 1993; Bendz-Hellgren and Stenlid 1998).

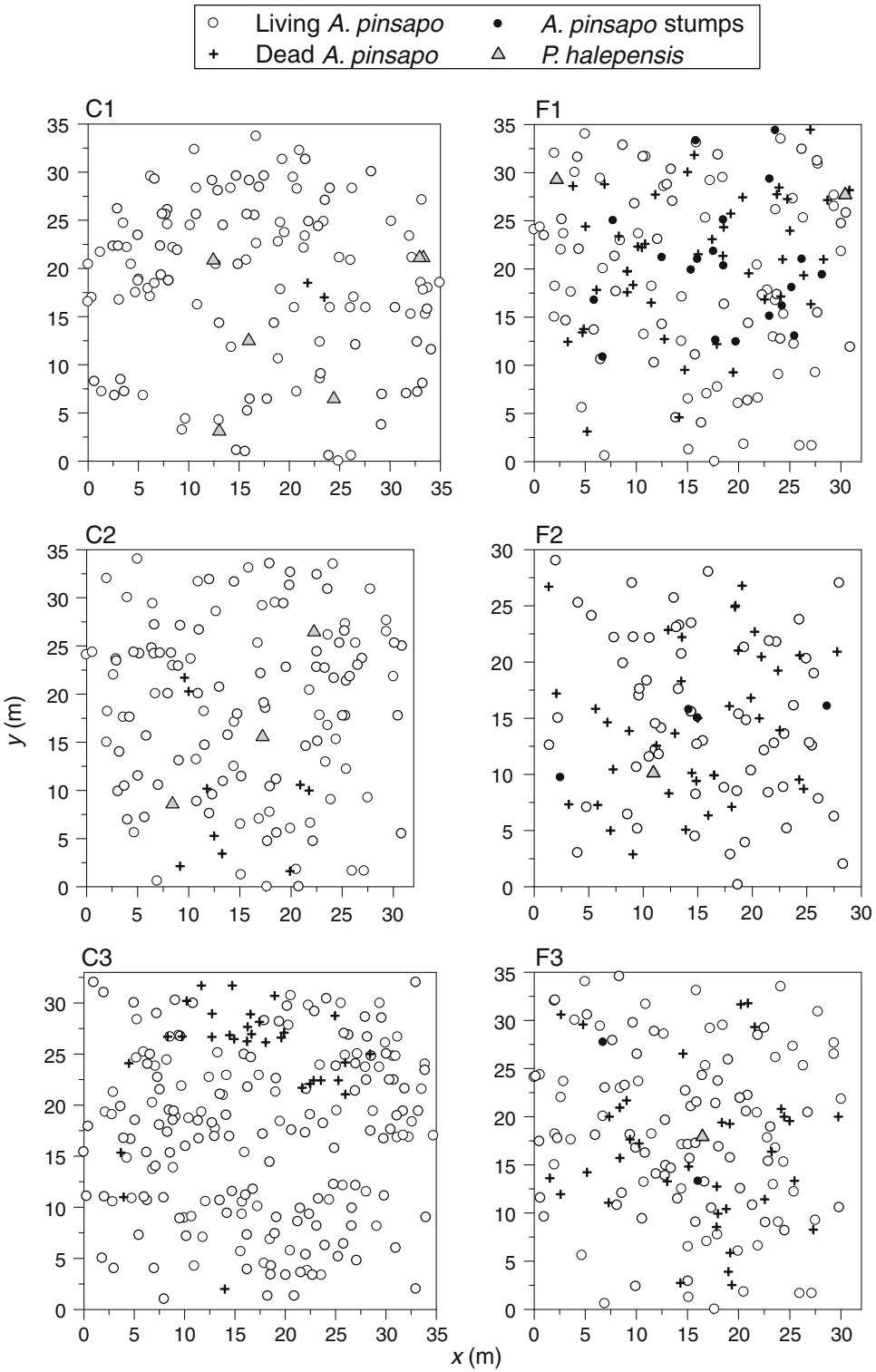

Fig. 2 Spatial patterns of *Abies pinsapo* trees in stands unaffected (plots *C1*, *C2* and *C3*) and affected (plots *F1*, *F2* and *F3*) by *Heterobasidion abietinum* root-rot disease. *Pinus halepensis* individuals are also shown. *White dots* living trees, *black dots* stumps, *crosses* dead trees, *grey triangles Pinus halepensis* trees

Notably, pathogens that cause increased damage in trees predisposed by stress are often already present in their host before the stressful event (Greig and Pratt 1976; Franklin et al. 1987; Manion 1991). The large size of some *H. abietinum* genets found in the study area suggests that they are more than 20 years old (Sánchez et al. 2007). Thus, their expansion began before the recurrent drought events in the early 1990s, when widespread *A. pinsapo* decline symptoms were first reported in the study area (Linares et al. 2009). We have previously shown that declining growth of trees that died between 1992 and 2001 began at the onset of the 1980s (Fig. 4). In addition, mortality was

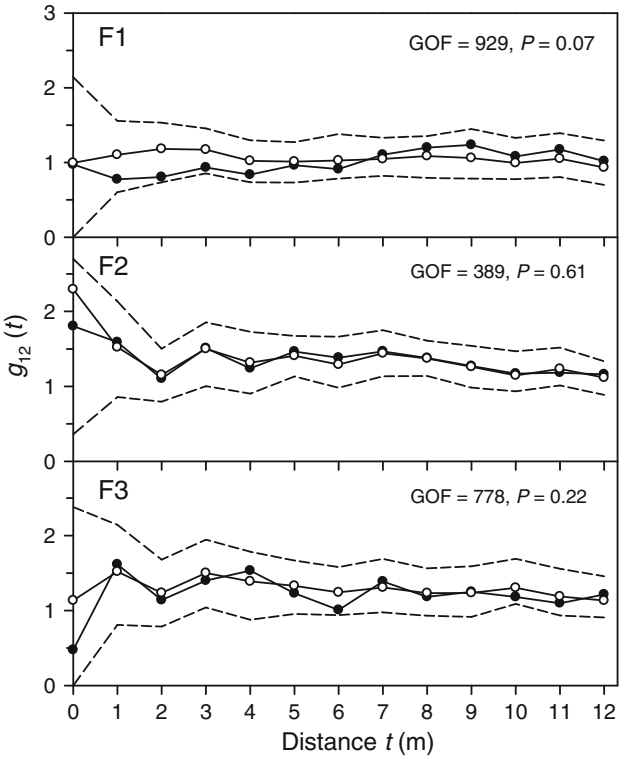

Fig. 3 Bivariate point-pattern analyses of living versus dead *Abies pinsapo* trees in three stands affected by *H. abietinum* root-rot disease (*F1*, *F2* and *F3*) based on the pair-correlation function ($g_{12}(t)$). The different lines correspond to the calculated $g_{12}(t)$ (*continuous line*, *filled symbols*) and expected $g_{12}(t)$ functions under the null model (*continuous line*, *empty symbols*) and the 5 and 95% simulation envelopes (*dashed lines*). Values of $g_{12}(t)$ greater or less than 1 indicate attraction or repulsion, respectively. The goodness-of-fit test (*GOF*) and its associated probability (*P*) summarise the deviation between the observed and simulated patterns, with higher values of GOF indicating stronger spatial patterns

related to preceding rainy years (1990, 1996 and 2001), which may have promoted *H. abietinum* expansion within tree hosts, followed by extreme drought years (1995, 1999 and 2005), which together with the long-term decline in rainfall may have caused the mortality of *A. pinsapo* (Figs. 4, 6; Linares et al. 2009, 2010).

Plant defences against pathogens involve the synthesis of biologically active secondary metabolites. However, plant pathology has usually emphasised the genetic regulation of host–pathogen interactions rather than the environmental regulation of a tree's ability to defend itself. Physiological status may determine whether a tree can withstand root-rot pathogens, and drought events influence tree growth and susceptibility to pathogens (Livingston et al. 1983; Desprez-Loustau et al. 2006). Indeed, the ability of drought to enhance fungal diseases in plants has been reported frequently, especially in forest trees (Castello et al. 1995; Cherubini et al. 2002; Puddu et al. 2003). Desprez-Loustau et al. (2006) found a positive drought-disease interaction in 56% of the references they reviewed regarding *Heterobasidion* species. Thus, we also expected a positive drought–disease relationship for *A. pinsapo* because drought events are strongly related to reduced growth. Similarly, we hypothesised that rainfall would favour *A. pinsapo* growth recovery, thereby promoting the synthesis of defence compounds and diminishing disease impact. However, we found an association between high mortality years and preceding periods of high rainfall (see Supplementary data).

Understanding the fundamental mechanisms underlying tree survival and mortality in the face of interacting drought and pathogen stresses requires knowledge of growth patterns and the physiological drivers of tree mortality (McDowell et al. 2008; Allen et al. 2010). Extreme drought events could induce *A. pinsapo* mortality through embolism and xylem cavitation (Zweifel et al. 2005). However, control plots showed much lower tree mortality than mortality-foci plots (Fig. 1), even though both were subjected to the same drought events and showed similar drought-related growth reductions (Fig. 4). This divergence illustrates the role of *H. abietinum* root-rot as a contributing factor to tree mortality. We explain this finding as a result of the decreased ability of root-damaged trees to cope with low soil-water availability. Thus, we hypothesise that trees in the F plots were killed by cavitation due to impaired or reduced water uptake due to fungal damage to tree roots. However, other interacting effects, as reduced nutrients uptake, are possible.

The death of roots, particularly roots that extract deep water from the soil, may be especially critical in sites with low water availability, such as Mediterranean forests (Desprez-Loustau et al. 2006). Furthermore, we hypothesise that, at a given level of root destruction by *H. abietinum*, the likelihood of growth decline and death will be higher in trees subjected to more intense competition (relatively smaller trees compared to the size and number of competing neighbours; see Supplementary data) than in dominant trees. Protracted water stress, caused by drought events and root damage by root-rot fungi, could drive larger carbon deficits and more severe growth and metabolic limitations in trees subjected to stronger neighbourhood competition (Linares et al. 2010).

Drought may interact with competition to predispose trees to be killed by *H. abietinum*. Our results suggest a likely sequence for *A. pinsapo* tree mortality that is consistent with existing conceptual models of tree disease dynamics (Manion 1991; McDowell et al. 2008; van Mantgem et al. 2009; Allen et al. 2010). Some infected trees are more stressed due to tree-to-tree competition combined with drought. This stressed state causes inadequate synthesis of secondary metabolites, declining growth and an inability to defend against the spread of root-rot. These conditions allow fungi to colonise and occlude the

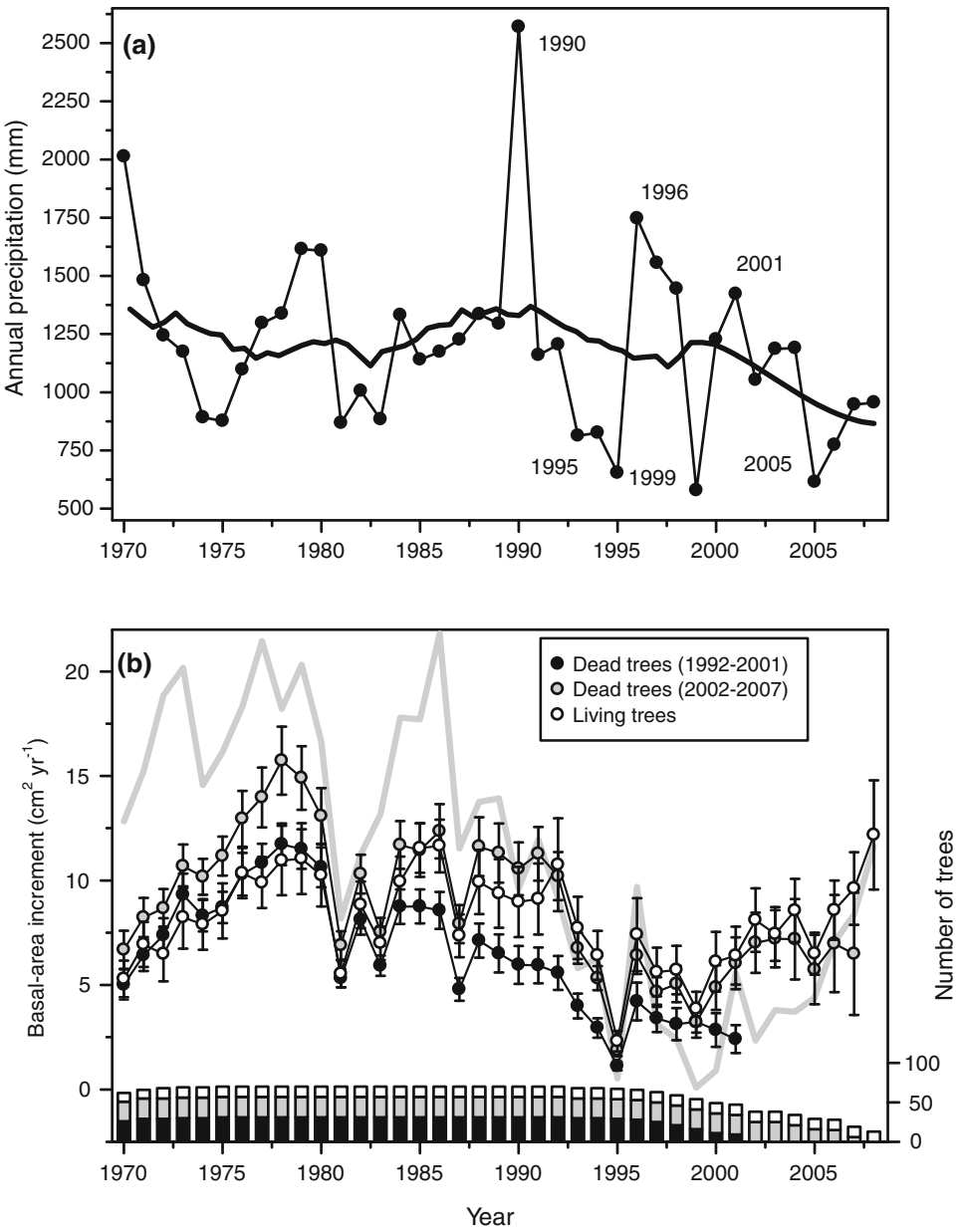

Fig. 4 Annual precipitation (**a**) and basal-area increment (**b**) trends. The *black line* (*top*) represents the long-term rainfall trend estimated by a local smoothing technique using polynomial regression and weights computed from the Gaussian density function (loess). Rainy years (1990, 1996 and 2001) followed by years with severe droughts (1995, 1999 and 2005) are noted. Basal-area increment data (*line*, *scattered points*) are represented separately for trees that died between 1992 and 2001 (*black symbols*) and between 2002 and 2007 (*grey symbols*) and for living trees in 2009 (*empty symbols*). The master basal-area increment series (*grey line*, *lower graph*) was obtained from dominant trees from the control plots (see also Linares et al. 2010). In the lower graph *error bars* represent standard errors and *bars* indicate annual sample size

sapwood more rapidly, causing transpiration to cease, which results in drying of the canopy and eventual tree death. The expansion of *H. abietinum* in *A. pinsapo* stands is further favoured by the dense and aggregated stand structure (Figs. 1, 2, 3) and the common occurrence of root contact and grafts in this fir species (Linares, personal observation), which enhance the formation of *Heterobasidion*-related mortality foci.

If the distance to foci is unimportant, is the fungus everywhere waiting for the right conditions?

The role of tree-to-tree competition as a predisposing stressor and as a factor that increases the chances of root contact and grafts among trees has received less attention than climate-driven effects (but see Olano et al. 2009). In this sense, our results indicate that the likelihood of growth decline and death is higher in trees subjected to more intensive competition (see Supplementary data) compared to dominant trees. Competition strongly modulates the adaptive capacity of *A. pinsapo* to withstand both long- and short-term climatic stressors (Linares et al. 2010). This result is important because it provides an understanding of decline and mortality processes in the context of both regional climatic trends and current root-rot pathogen dynamics. Our results also highlight the need to incorporate canopy-structural and density-dependent factors into conceptual frameworks to assess the vulnerability of forest ecosystems to climate change.

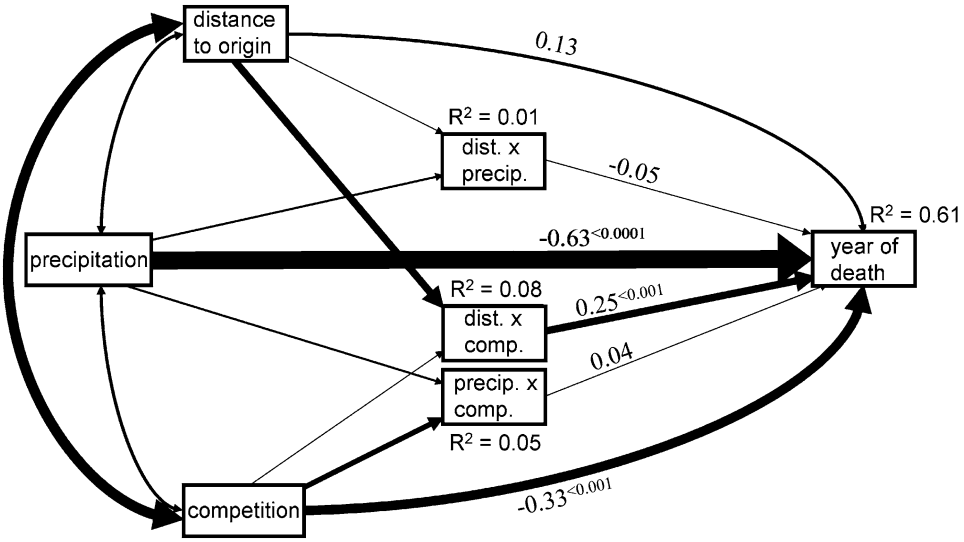

Fig. 5 Final "best" structural equation model, selected using AIC. *Boxes* represent measured variables, *directed arrows* (paths) represent a causal influence, and *bidirectional arrows* represent an undirected correlation. Path coefficients, indicating the estimated strength of one variable's influence on another appear next to the arrows which are central to the hypotheses considered here, and *arrow* width is scaled proportionately. If less than 0.10, associated probability values appear as *superscripts*. Path coefficients for correlations among main effects, and for effects of main effects upon their interaction terms are omitted for simplicity. R^2 is proportion of variance explained and is interpreted similarly to a regression analysis; each response variable has a unique R^2

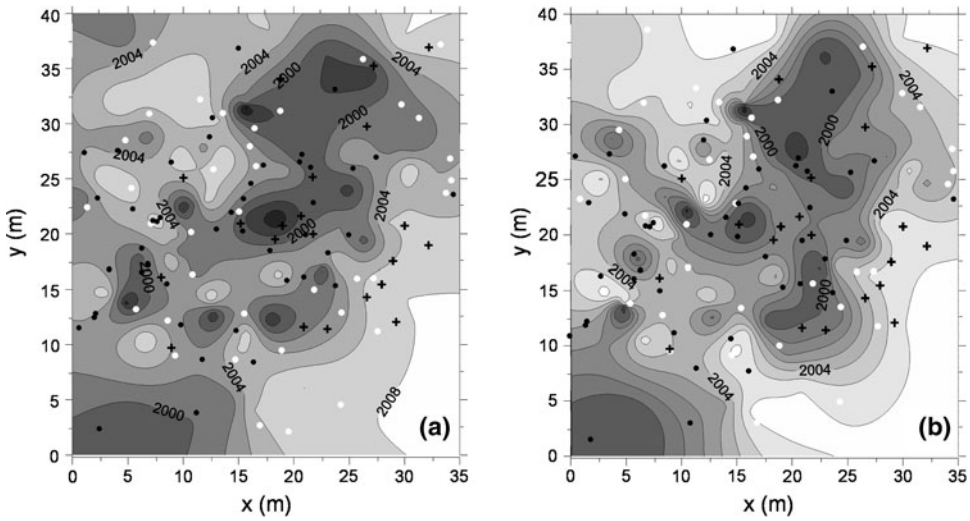

Fig. 6 Observed (**a**) and SEM-predicted (**b**) year of tree death (last tree-ring formed). Death dates were interpolated using kriging with *darker* (*clearer*) *colours* indicating earlier (later) death dates. *Crosses* stumps, *black dots* dead trees, *white dots* living trees

Heterobasidion-caused root-rot generally occurs more frequently in managed than in relatively undisturbed forests, where the fungus seldom causes significant damage at the stand level (Korhonen and Stenlid 1998; Stenlid and Redfern 1998). However, this fungus has been cited recently as a concurrent factor in the decline of weakly managed *A. alba* stands in the Spanish Pyrenees (Camarero 2000). Likewise, *H. abietinum* has become a relatively virulent pathogen in natural *A. pinsapo* forests, causing root and butt rot in living trees and forming disease gaps and mortality foci (Sánchez et al. 2005). These gaps are being colonised by *A. pinsapo*, *Quercus ilex* L. subsp. *rotundifolia*, *Q. faginea* Lam. and *Pinus halepensis* Mill., favouring the replacement of pure *A. pinsapo* with mixed stands.

Regional land-use changes may have exacerbated recent stand stagnation and mortality in many forests (Lindner et al. 2009; Linares et al. 2009, 2010; Allen et al. 2010). In portions of southern Spain, over half a century of forest recovery and protection has fostered the development of unusually dense and highly clustered stands. Tree populations in these dense forests, excluded from traditional uses (e.g. logging), may have undergone a decrease in their capacity to adapt to stressors, making them more vulnerable to the interactive effects of drought and fungal pathogens. Land use changes have been linked to recent

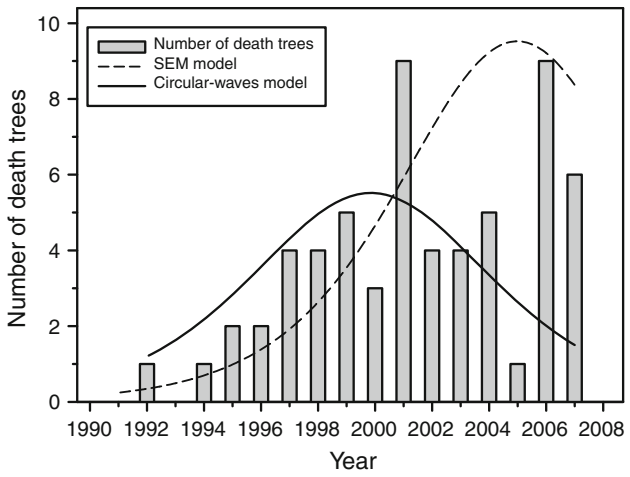

Fig. 7 Annual mortality rates for *Abies pinsapo* affected by *Heterobasidion abietinum* root-rot. The *continuous line* represents the mortality frequency predicted by the simple distance-dependent "circular-waves" model (see Fig. 5). The *dotted line* represents the mortality frequency predicted by the final "best" structural equation model (*SEM*) (see also Figs. 5, 6)

growth declines and mortality in currently protected Spanish populations that were intensively used for logging and grazing in the past (Linares et al. 2009; Linares and Carreira 2009). In addition, a greater incidence of *H. abietinum* leaded to suggest that global warming may be increasing the vulnerability of *A. pinsapo* to root-rot disease, thus exacerbating the decline of this relict fir species (Sánchez et al. 2005, 2007). However, our result shows that precipitation variability and land-use-related stand structure changes, instead of temperature increase, are more related to enhancing *H. abietinum* incidence.

Conclusions

Our results could have broad implications by highlighting the need for improved researches and methods that combine disease vectors and stand structure. *A. pinsapo* tree mortality involves the concurrence of multiple interacting factors, ranging from trends in mean and extreme climatic conditions to stand-structural features and root-rot disease dynamics. Drought conditions seem to be an inciting factor, triggering a sudden growth reduction and a sharp rise in mortality in trees that are already stressed by both competition and root-rot damage, which act as predisposing factors. Our results indicate that trees that are infected by *Heterobasidion* and subjected to more intensive competition have a reduced ability to withstand water-deficit stress, as indicated by their lower basal-area increments and greater growth reduction in response to drought spells. This study demonstrates that competition may also lead to declining growth and a reduced ability to overcome further extreme climatic events, such as new severe droughts. It is likely that, under some plausible scenarios, warming will induce more rapid spread of fungal pathogens, resulting in significant decline and mortality episodes of remnant *A. pinsapo* populations. In summary, given the existing high incidence of *H. abietinum* in *A. pinsapo* forests and the potential risks of warming-induced *A. pinsapo* die-off, forest managers must develop adaptive strategies to improve the resistance and resilience of these relict Mediterranean fir forests to projected increases in climatic stress. Management options include thinning stands to reduce competition and enhance spatial heterogeneity. Stand thinning will also favour the establishment of co-occurring *Quercus* species. Alternatively, *Quercus* individuals might be deliberately introduced, thereby accelerating succession from pure *A. pinsapo* forests towards mixed stands co-dominated by other tree species that are not affected by *H. abietinum.*

Acknowledgments This study was supported by projects PP06-RNM-02183 (Consejería de Innovación y Ciencia, Junta de Andalucía) and REN2002-2003-09509 (Spanish Ministry of Science). J.J.C. is grateful for the support of ARAID and the Globimed network. Tree cutting was supported by the Consejería de Medio Ambiente, Junta de Andalucía, with the helpful collaboration of J. López Quintanilla. We thank Dr. E. Sánchez for insightful discussions and G. Sangüesa for valuable laboratory assistance. We also thank Ram Oren and two anonymous reviewers for their helpful comments. These experiments comply with the current laws of Spain.

References

Allen CD, Macalady AK, Chenchouni H, Bachelet D, McDowell N, Vennetier M, Kitzberger T, Rigling A, Breshears DD, Hogg EH, Gonzalez P, Fensham R, Zhang Z, Castro J, Demidova N, Lim J-H, Allard G, Running SW, Semerci A, Cobb N (2010) A global overview of drought and heat-induced tree mortality reveals emerging climate change risks for forests. For Ecol Manage 259:660–684

Ayres MP, Lombardero MJ (2000) Assessing the consequences of global change for forest disturbance from herbivores and pathogens. Sci Total Environ 262:263–286

Bendz-Hellgren M and Stenlid J (1998) Effects of clear-cutting, thinning, and wood moisture content on the susceptibility of Norway spruce stumps to *Heterobasidion annosum.* Can J For Res 28:759–765

Burnham KP, Anderson DR (2001) Kullback–Leibler information as a basis for strong inference in ecological studies. Wildl Res 28:111–119

Burnham KP, Anderson DR (2002) Model selection and multimodel inference, 2nd edn. Springer, New York

Camarero JJ (2000) El decaimiento del abeto en los Pirineos. Medio Ambiente Aragón 4:18–20

Castello JD, Leopold DJ, Smallidge PJ (1995) Pathogens, patterns, and processes in forest ecosystems. Bioscience 45:16–24

Cherubini P, Fontana G, Rigling D, Dobbertin M, Brang P, Innes JL (2002) Tree-life history prior to death: two fungal root pathogens affect tree-ring growth differently. J Ecol 90:839–850

Das A, Battles J, van Mantgem PJ, Stephenson NL (2008) Spatial elements of mortality risk in old-growth forests. Ecology 89:1744–1756

Desprez-Loustau ML, Marcais B, Nageleisen LM, Piou D, Vannini A (2006) Interactive effects of drought and pathogens in forest trees. Ann For Sci 63:597–612

Diggle PJ (2003) Statistical analysis of point patterns. Arnold, London

Dobbertin M, Baltensweiler A, Rigling D (2001) Tree mortality in an unmanaged mountain pine (*Pinus mugo* var. uncinata) stand in the Swiss National Park impacted by root rot fungi. For Ecol Manage 145:79–89

Franklin JF, Shugart HH, Harmon ME (1987) Tree death as an ecological process. Bioscience 37:550–556

Goreaud F, Pèlissier R (2004) Avoiding misinterpretation of biotic interactions with the intertype K_{12}-function: population independence vs. random labeling hypotheses. J Veg Sci 14:681–692

Grace JB (2006) Structural equation modeling and natural systems. Cambridge University Press, Cambridge

Greig BJW, Pratt JE (1976) Some observations on the longevity of *Fomes annosus* in conifer stumps. Eur J For Path 6:250–253

Hegyi F (1974) A simulation model for managing jack-pine stands. In: Fries J (ed) Growth models for tree and stand simulation. Royal College of Forestry, Stockholm, Sweden, pp 74–90

Holdenrieder O, Pautasso M, Weisberg PT, Lonsdale D (2004) Tree diseases and landscape processes: the challenge of landscape pathology. Trends Ecol Evol 19:446–451

Holmes RL (1983) Computer-assisted quality control in tree-ring dating and measurement. Tree Ring Bull 43:68–78

Holmes RL (1992) Dendrochronology program library. Laboratory of Tree-Ring Research, University of Arizona, Tucson

Kline TJB, Dunn B (2000) Analysis of interaction terms in structural equation models: a non-technical demonstration using the deviation score approach. Can J Behav Sci 32:127–132

Korhonen K, Stenlid J (1998) Biology of *Heterobasidion annosum*. In: Woodward S, Stenlid J, Karjalainen R, Hiittermann A (eds) *Heterobasidion annosum*: biology, ecology, impact and control. CAB International, Wallingford, pp 43–70

Lacey L (1986) Water availability and fungal reproduction: patterns of spore production, liberation and dispersal. In: Ayres PG, Boddy L (eds) Water, fungi and plants. Cambridge University Press, Cambridge, pp 65–86

Lewis KJ, Lindgren BS (1999) Influence of decay fungi on species composition and size class structure in mature *Picea glauca x engelmannii* and *Abies lasiocarpa* in sub-boreal forests of central British Columbia. For Ecol Manage 123:135–143

Linares JC and Carreira JA (2009) Temperate-like stand dynamics in relict Mediterranean-fir (*Abies pinsapo*, Boiss.) forests from Southern Spain. Ann For Sci 66

Linares JC, Camarero JJ, Carreira JA (2009) Interacting effects of climate and forest-cover changes on mortality and growth of the southernmost European fir forests. Glob Ecol Biogeogr 18:485–497

Linares JC, Camarero JJ, Carreira JA (2010) Competition modulates the adaptation capacity of forests to climatic stress: insights from recent growth decline and death in relict stands of the Mediterranean fir *Abies pinsapo*. J Ecol 98:592–603

Lindberg M, Johansson M (1992) Resistance of *Picea abies* seedlings to infection by *Heterobasidion annosum* in relation to drought stress. Eur J For Path 22:115–124

Lindner M, Maroschek M, Netherer S, Kremer A, Barbati A, Garcia-Gonzalo J, Seidl R, Delzon S, Corona P, Kolström M, Lexer M, Marchetti M (2009) Climate change impacts, adaptive capacity, and vulnerability of European forest ecosystems. For Ecol Manage 162:73–86

Liu D, Kelly M, Gong P, Guo Q (2007) Characterizing spatial-temporal tree mortality patterns associated with a new forest disease. For Ecol Manage 253:220–231

Livingston W, Mangini A, Kinzer H, Mielke M (1983) Association of root diseases and bark beetles Coleoptera: Scolytidae. with *Pinus ponderosa* in New Mexico, USA. Plant Dis 67:674–676

Lonsdale G, Gibbs JN (1996) Effects of climate change on fungal diseases of trees. In: Frankland JC, Magan N, Gadd GM (eds) Fungi and environmental change. Cambridge University Press, Cambridge, pp 1–19

Manion PD (1991) Tree disease concepts. Prentice-Hall, Englewood Cliffs

McDowell N, Pockman WT, Allen CD, Breshears DD, Cobb N, Kolb T, Sperry J, West A, Williams D, Yepez EA (2008) Mechanisms of plant survival and mortality during drought: why do some plants survive while others succumb to drought? New Phytol 178:719–739

Olano JM, Laskurain NA, Escudero A, De La Cruz M (2009) Why and where do adult trees die in a young secondary temperate forest? The role of neighbourhood. Ann For Sci 66:105–112

Orwig DA, Abrams MD (1997) Variation in radial growth responses to drought among species, site, and canopy strata. Trees Struct Funct 11:474–484

Peet RK, Christensen NL (1987) Competition and tree death. Bioscience 37:586–594

Puddu A, Luisi N, Capretti P, Santini A (2003) Environmental factors related to damage by *Heterobasidion abietinum* in *Abies alba* forests in Southern Italy. For Ecol Manage 180:37–44

Rayner ADM (1986) Water and the origins of decay in trees. In: Ayres PG, Boddy L (eds) Water, fungi and plants, Cambridge University Press, Cambridge, pp 321–341

Redfern DB (1993) The effect of wood moisture on infection of Sitka spruce stumps by basidiospores of *Heterobasidion annosum*. Eur J For Path 23:218–235

Sánchez ME, Capretti P, Calzado C, Navarro Cerrillo RM, Trapero A (2005) Root rot disease on *Abies pinsapo* in southern Spain. In: Manka M, Lakomy P (eds) Proc 11th Int Conf Root and Butt Rots, 16–22 August 2004, IUFRO. The August Ciezuowski, Agricultural University, Poznan, Poland, pp 220–223

Sánchez ME, Luchi N, Jiménez JJ, de Vita P, Sánchez JE, Trapero A, Capretti P (2007) An isolated population of *Heterobasidion abietinum* on *Abies pinsapo* in Spain. For Pathol 37:348–356

Solla A, Camarero JJ (2006) Spatial patterns and environmental factors affecting the presence of *Melampsorella cariophyllacearum* infections in an *Abies alba* forest in NE Spain. For Pathol 36:165–175

Stenlid J, Redfern DB (1998) Spread within the tree and stand. In: *Heterobasidion annosum*: biology, ecology, impact and control. CAB International, Wallingford, Oxon, pp 125–141

Stoyan D, Stoyan H (1994) Fractals, random shapes and point fields: methods of geometrical statistics. Wiley, Chichester

van Mantgem PJ, Stephenson NL, Byrne JC, Daniels LD, Franklin JF, Fulé PZ, Harmon ME, Larson AJ, Smith JM, Taylor AH, Veblen TT (2009) Widespread increase of tree mortality rates in the western United States. Science 323:521–524

Wiegand T, Moloney KA (2004) Ring, circles, and null-models for point pattern analysis in ecology. Oikos 104:209–229

Zweifel R, Zimmermann L, Newbery DM (2005) Modeling tree water deficit from microclimate: an approach to quantifying drought stress. Tree Physiol 25:147–156

Electronic supplementary data.

Table S1. Characteristics of the meteorological stations used to compute the regional mean climatic series.

Station	Latitude (N)	Longitude (W)	Elevation (m a.s.l.)	Years for precipitation data	Mean annual precipitation (mm)	Years for temperature data	Mean annual temperature (ºC)
Alozaina	36º 43’ 40’’	04º 51’ 24’’	386	1955–2003	602	1977–2003	18.6
Casarabonela	36º 47’ 00’’	04º 50’ 24’’	480	1954–2003	808	1966–1981	16.7
El Burgo	36º 47’ 20’’	04º 56’ 43’’	591	1949–2003	615	1966–2003	15.2
Yunquera	36º 43’ 56’’	04º 55’ 13’’	681	1966–1984	640	—	—
Grazalema	36º 45’ 34’’	05º 22’ 01’’	823	1913–2003	2011	1964–2003	15.4
Quejigales	36º 41’ 20’’	05º 02’ 51’’	1100	1983–2001	1167	1983–2001	10.8

Table S2. Results of structural equation model selection and path estimation of model alternatives: k = number of parameters, AIC = Akaike's Information Criterion. Additional columns represent specific paths in the models and the variance in year of death explained by each model (R^2). The best model is indicated in bold. Alternative models are described in the text.

	k	AIC	distance → year of death	precipitation → year of death	competition → year of death	dist. × precip. → year of death	dist. × comp. → year of death	precip. × comp. → year of death	R^2- year of death
independence	16	117.919	0	0	0	0	0	0	0
null	17	118.272	0.13	0	0	0	0	0	0.02
distance-precipitation	19	78.002	0.19	-0.67	0	-0.07	0	0	0.47
distance-competition	19	106.143	0.04	0	-0.42	0	0.26	0	0.22
main effects	19	67.516	0.07	-0.63	-0.31	0	0	0	0.54
global	**22**	**61.242**	**0.13**	**-0.63**	**-0.33**	**-0.05**	**0.25**	**0.05**	**0.61**
P-values (best model)			0.112	<0.001	< 0.001	0.49	<0.001	0.559	

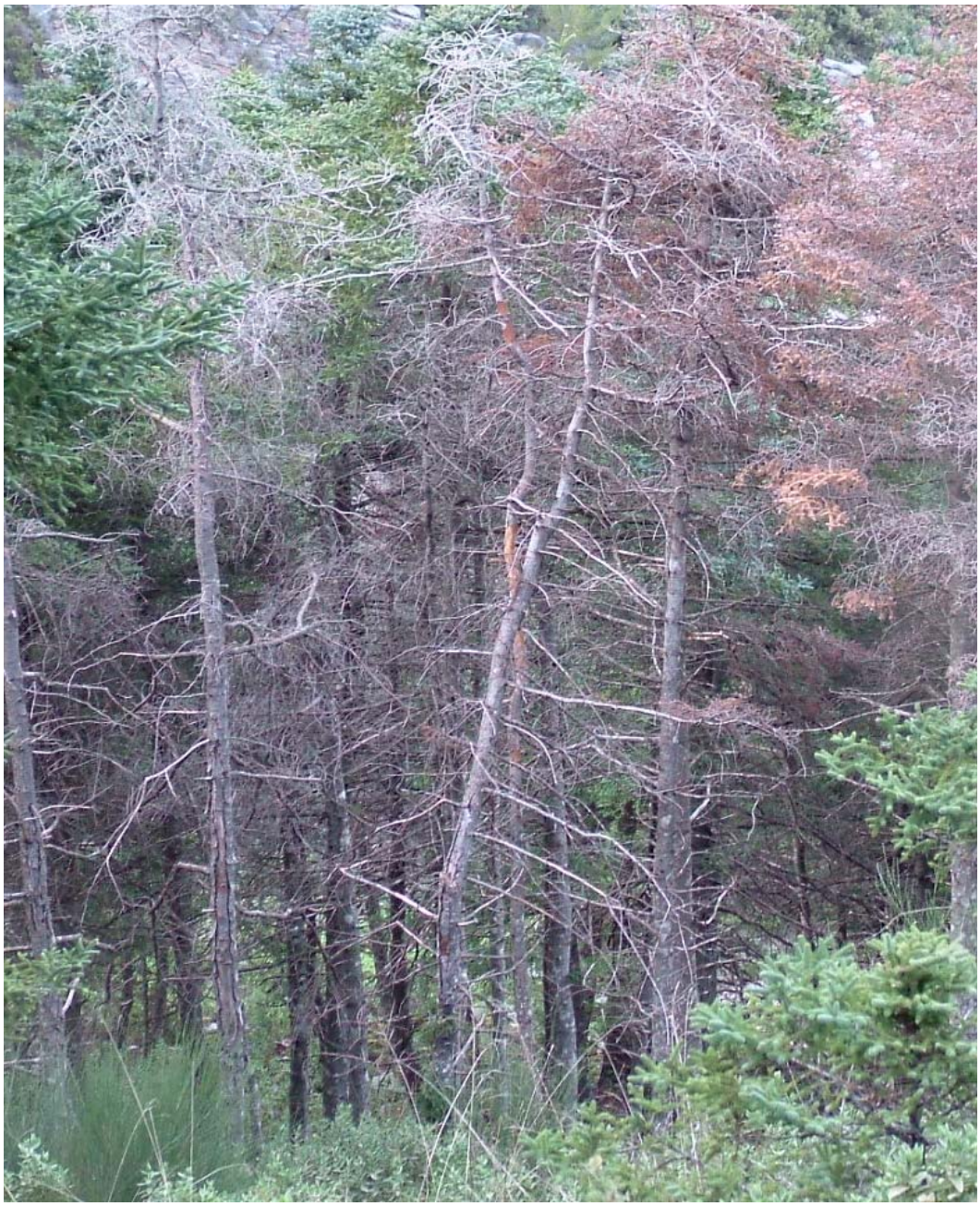

Figure S1. Standing dead *A. pinsapo* trees affected by *Heterobasidion abietinum* root rot (Photograph by J.C. Linares). In 2005, *H. abietinum* root rot was estimated to affect ca. 10% of *A. pinsapo* trees growing between 1000 and 1200 m in forests in the study area, but the incidence of the disease decreased above 1200 m (information provided by forest guards and managers of the Sierra de las Nieves Natural Park; see also Linares et al. (2009)). In field surveys carried out in *A. pinsapo* forests in 2002, a total of 72 disease foci were located within an area of about 3000 ha of fir forests in Sierra de las Nieves Natural Park Navarro et al. (2003). Before 1990, this pathogen was not considered an important mortality agent in these *A. pinsapo* forests Ruiz de la Torre et al. (1994).

Figure S2. Windthrown *A. pinsapo* trees affected by *Heterobasidion abietinum* root rot (Photographs taken in the plot F1 by V. Ochoa).

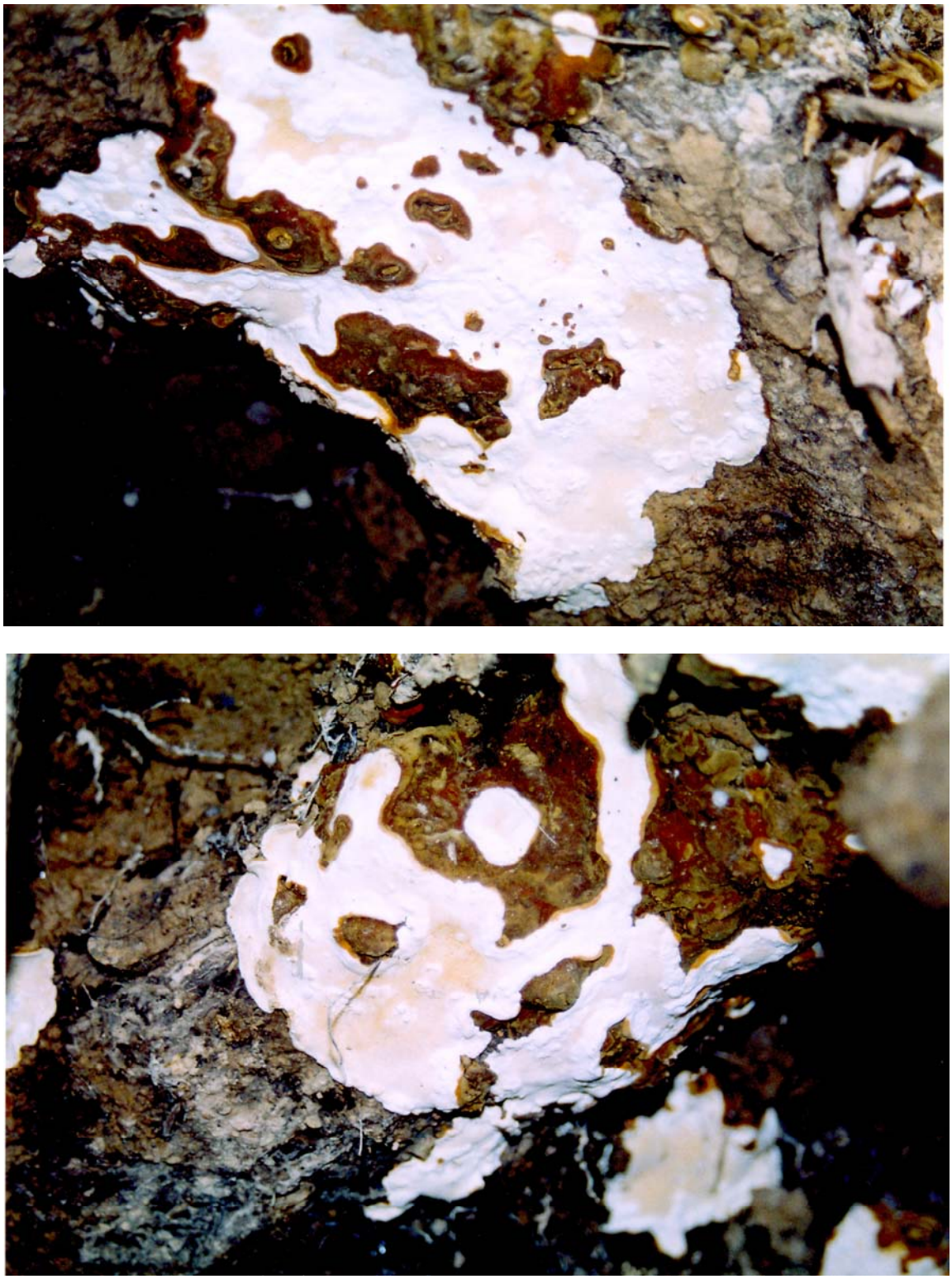

Figure S3. Fruiting bodies of *Heterobasidion abietinum* found in the primary-root system of windthrown *A. pinsapo* trees in the surveyed disease foci (Photographs by J.C. Linares).

Figure S4. Old *A. pinsapo* stump affected by *Heterobasidion abietinum* root rot in the surveyed disease foci (Photograph by J.C. Linares).

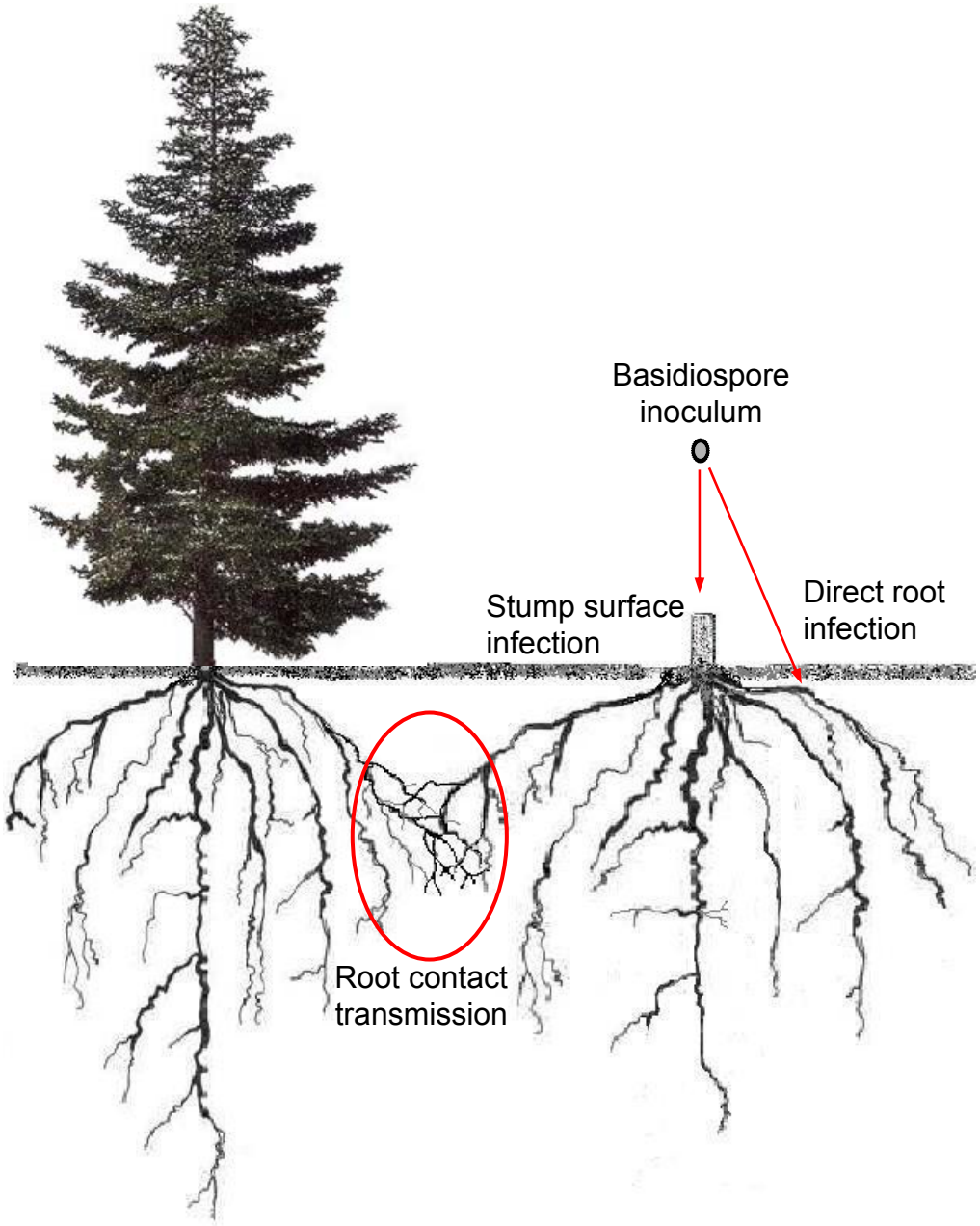

Figure S5. General scheme of *Heterobasidion s.l.* infection and dispersal. *Heterobasidion s.l.* disease origin occurs mainly by airborne basidiospores that germinate on fresh stump or stem or on root surface wounds of living trees. From this primary foci, disease dispersal occur mainly by direct growth of the pathogen from tree to tree through root contacts or grafts, and therefore spatial disease pattern could be modelled as a function of tree distance to the older infection point. Stumps generated 20 years ago in the *A. pinsapo* forest were not treated to protect against aerial infection by *H. abietinum*. However, recent infections related to felling are less likely because the stumps were treated. Nowadays, growth of *H. abietinum* through root contacts or grafts from tree to tree appears to be the most likely route for the spread of infection.

Figure S6. Stem wounds (top of the image) likely due to rock detachment. *Heterobasidion s.l.* spreads can occurs by airborne basidiospores that germinate on fresh stump but also on this kind of stem or root wounds of living trees (Photograph by J.J. Camarero).

Figure S7. Round holes and galleries found in the stems of some root-rot affected *A. pinsapo* trees. Scolytids as the bark beetle *Cryphalus numidicus* Eich. (COLEOPTERA, *Scolitiydae*); cerambycids as the wood boring beetle *Ergates faber* L. (COLEOPTERA, *Cerambicydae*), and hymenopters as the carpenter bee *Xylocopa violacea* L. (HYMENOPTERA, *Anthophoridae*) were established in the stems (Photographs by J.C. Linares).

Figure S8. Standing and windthrow *A. pinsapo* trees in the plot F1 (Photograph by V. Ochoa). In *H. abietinum* foci, root rot causes mortality and increases the incidence of windthrown trees. Fruit bodies identified as *H. abietinum* (see Sánchez et al. (2007)) were detected on windthrown trees and old stumps in the study site. *Heterobasidion* species are spread by airborne basidiospores, which germinate on fresh stumps or on surface wounds on the stems and roots of living trees. Infection of neighbouring trees takes place via root contact (see Stenlid & Redfern (1998)). In stumps, *Heterobasidion* can remain active for up to 62 years Greig & Pratt (1976); Stenlid & Redfern (1998).

Figure S9. Windthrow *A. pinsapo* tree affected by *Heterobasidion abietinum* root rot (Photograph by V. Ochoa).

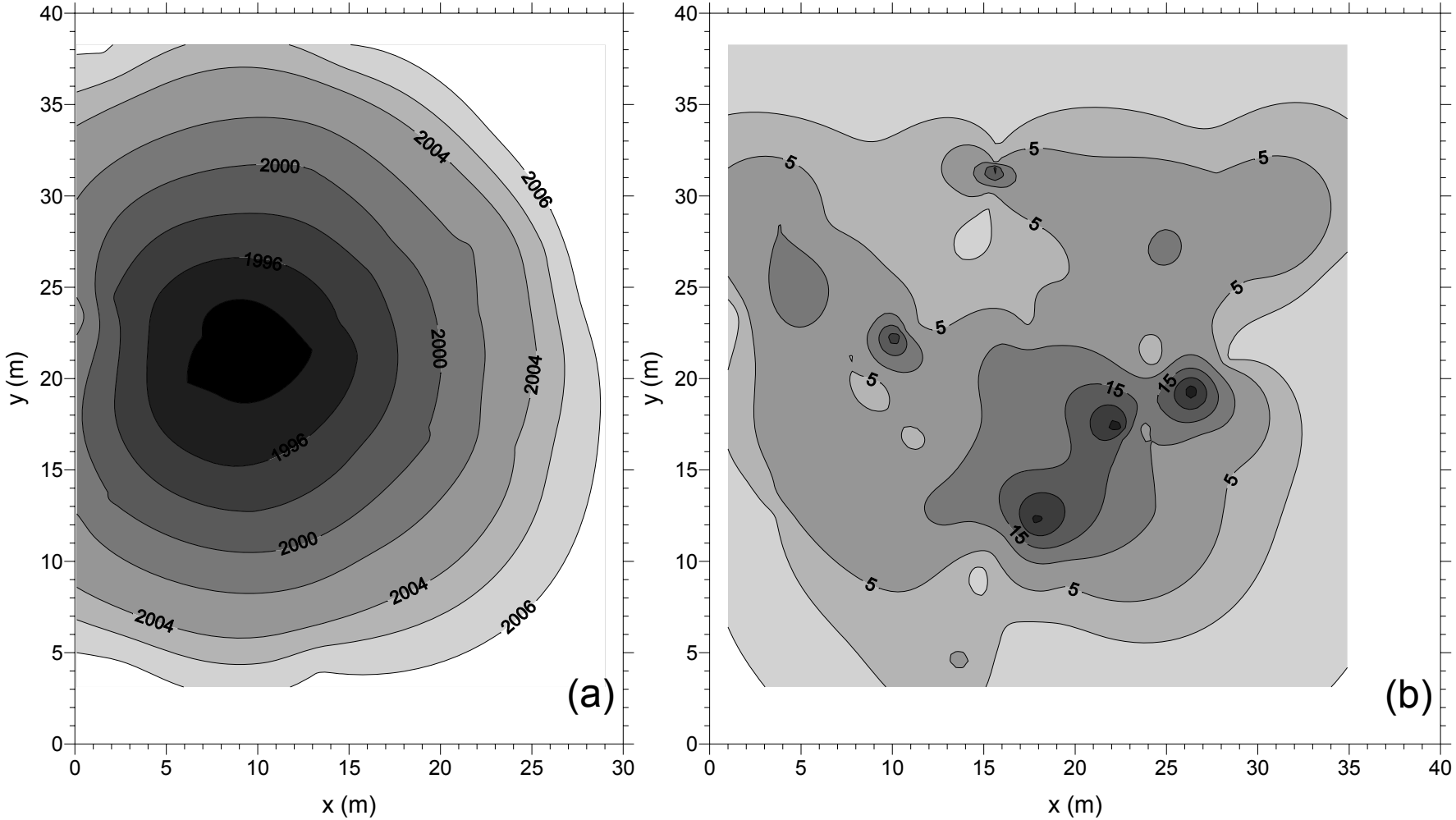

Figure S10. Predicted year of tree death (last tree-ring formed) by circular wave model (a) and observed competition-index (b). The model (a) was evaluated as null hypothesis using the distance to the origin foci as predictor; competition intensity was evaluated as alternative predictor.

Supplementary References

Greig BJW, Pratt JE (1976) Some observations on the longevity of *Fomes annosus* in conifer stumps. Eur. J. For. Path. 6:250-253

Linares JC, Camarero JJ, Carreira JA (2009) Interacting effects of climate and forest-cover changes on mortality and growth of the southernmost European fir forests. Glob. Ecol. Biogeogr. 18:485-497

Navarro RM, Calzado C, Sánchez ME, López J, Trapero A (2003) Censo de focos de *Heterobasidion annosum* (Fr.) Bref. en ecosistemas de pinsapo. Bol. Sanid. Veg. , Plagas 29:581-592

Ruiz de la Torre J, García JI, Oria de Rueda JA, Cobos JM, Neva JC, Navarro Cerrillo RMª, Catalina MA, López-Quintanilla J, Alvarez Calvente M, Arista M, Talavera S, Herrera J (1994) Gestión y conservación de los pinsapares andaluces. Asociación forestal andaluza,

Sánchez ME, Luchi N, Jiménez JJ, de Vita P, Sánchez JE, Trapero A, Capretti P (2007) An isolated population of *Heterobasidion abietinum* on *Abies pinsapo* in Spain. For. Path. 37:348-356

Stenlid J, Redfern DB (1998) Spread within the tree and stand. In: Heterobasidion annosum: Biology, Ecology, Impact and Control. Wallingford, Oxon, UK: CAB International, pp. 125-141.,